

**Properties of *in situ* polymerized  
poly(3,4-ethylenedioxythiophene)/alumina  
composites for energy storage applications**

**Mari Cruz G. Saborío,<sup>1,2</sup> Frances Estrany,<sup>1,2,\*</sup> and Carlos  
Alemán<sup>1,2,\*</sup>**

<sup>1</sup> *Departament d'Enginyeria Química, EEBE, Universitat Politècnica de Catalunya, C/ Eduard Maristany, 10-14, Ed. I2, 08019, Barcelona, Spain*

<sup>2</sup> *Barcelona Research Center for Multiscale Science and Engineering, Universitat Politècnica de Catalunya, Eduard Maristany, 10-14, 08019, Barcelona, Spain*

\* [francesc.estrany@upc.edu](mailto:francesc.estrany@upc.edu) and [carlos.aleman@upc.edu](mailto:carlos.aleman@upc.edu)

## **ABSTRACT**

Composites formed by poly(3,4-ethylenedioxythiophene) and alumina (PEDOT/Al<sub>2</sub>O<sub>3</sub>) have been prepared by in situ anodic polymerization. For this purpose, the stability of 1:1 and 4:1 monomer:alumina aqueous solutions has been examined as a function of the pH (2.3, 4.0, 7.0, 8.8 or 10.8). Results indicate that the monomer behaves as a dispersant that remains stable at the studied basic pHs despite they are close to the isoelectric point of alumina. Although the thermal stability of the composites is considerably affected by the pH of the reaction medium, its influence on the surface morphology is very small. Independently of the synthetic conditions, the electrochemical properties were better for PEDOT/Al<sub>2</sub>O<sub>3</sub> than for pure PEDOT, reflecting that alumina particles promote the charge mobility. The highest specific capacitance (141 F/g), which was 55% higher than that obtained for pure PEDOT, was achieved for the composite prepared at pH= 8.8 using a 4:1 monomer:alumina ratio. These conditions favour the participation of OH<sup>-</sup> groups as secondary doping agents without degrading the polymer matrix and enhance the specific surface of the films, facilitating the ionic mobility. On the other hand, application of a multi-step polymerization strategy has shown that interfaces originated by consecutive steps enhance the specific capacitance.

**Keywords:** Al<sub>2</sub>O<sub>3</sub>; charge mobility; conducting polymer; multilayers; polythiophene

## INTRODUCTION

Due to their large capacitance, good electric conductivity, ease of synthesis and low cost, intrinsic conducting polymers (ICPs) are currently considered as mature industrial products for the fabrication of energy storage devices with parallel development activities at the research laboratory level.<sup>1-6</sup> The most commonly used ICPs are polyaniline (PAni), polypyrrole (PPy), and poly(3,4-ethylenedioxythiophene) (PEDOT) and their derivatives. Through chemical or electrochemical processes, most ICPs can be synthesized by oxidization of the corresponding monomer in solution.<sup>7</sup> The conductivity and capacitance of these ICPs can be tuned through the dopant, the level of doping and/or the fabrication of a (nano)composite by adding another electroactive material.

Among ICPs, poly(3,4-ethylenedioxythiophene) (PEDOT) has been widely used for the fabrication of energy storage devices because of its outstanding capacitive performance, fast doping-undoping process, stable charge-discharge response, high conductivity, good environmental stability in its doped state, relative ease of preparation, and advantages in cost.<sup>8-13</sup> Furthermore, the capacitive and electrochemical properties of PEDOT have been enhanced forming hybrid nanocomposites through its combination with other materials, as for example with clays,<sup>10</sup> graphene,<sup>14,15</sup> carbon nanotubes,<sup>16</sup> inorganic oxides,<sup>17,18</sup> and even biopolymers.<sup>19,20</sup>

Aluminium oxide ( $\text{Al}_2\text{O}_3$ ), commonly named alumina, represents an attractive material to be used for the fabrication of PEDOT-based electrodes with enhanced electrochemical properties. This ceramic material exhibits noticeable features, as for example, low-cost, availability, non-toxicity and, most importantly, its surface properties in suspensions can be tuned with the pH. Thus, surface hydroxyl groups of alumina may react with acid and base at low and high pH, respectively, to form positive and negative charges, respectively, while the alumina surface sites are neutral when the

isoelectric point is reached at  $\text{pH} = 9.2$ .<sup>21</sup> Thus, the pH-induced interfacial charging properties of alumina are expected to be a powerful tool to regulate the characteristics of the PEDOT- and alumina-containing composites (PEDOT/ $\text{Al}_2\text{O}_3$ ).

In absence of dispersant, aqueous suspensions of alumina particles exhibit colloidal stability at pHs ranging from 3 and 7.8, in which the potential repulsion produced by charged particles preclude aggregation phenomena (*i.e.* van der Waals attraction is overwhelmed).<sup>22</sup> In contrast, van der Waals attraction dominates the total particle–particle interaction when the charge decreases or disappears at the isoelectric point, leading to coagulation of particles in the suspension. Accordingly, the sign and magnitude of the charge onto the alumina particle surface will control, at least partially, the interaction of the alumina with polymer chains. On the other hand, it has been reported that acidification affects the oxidative polymerization of PEDOT. More specifically, protic and Lewis acids were found to catalyse an equilibrium reaction of 3,4-ethylenedioxythiophene (EDOT) monomers to the corresponding dimeric and trimeric species without further oxidation reaction.<sup>23</sup>

Porous alumina membranes with a pore diameter of  $\sim 200$  nm and a thickness of  $\sim 6$   $\mu\text{m}$  have been used as a template for the electrochemical synthesis of PEDOT nanotubes<sup>24-27</sup> using an approach based on the pioneering procedure proposed by Martin and co-workers two decades ago.<sup>28-30</sup> Indeed, alumina membranes offer advantages as a template over conventional polycarbonate track-etched membranes, such as higher pore density and well-ordered pore structure.<sup>31</sup> However, in spite of their enormous potential for energy storage applications, the electrochemical synthesis of PEDOT/ $\text{Al}_2\text{O}_3$  in acidic or basic conditions have not explored yet and the properties of the resulting composites are unknown.

On the other hand, in recent studies we investigated the properties of multi-layered systems formed by alternated layers of PEDOT and other ICPs.<sup>8,32-35</sup> We found that such multi-layered composites, which were prepared using the layer-by-layer electrodeposition technique, present higher electrochemical activity and specific capacitance (*SC*) than each of the individual ICPs. This improvement was attributed to the synergistic effects produced by both the favourable interactions and the porosity increment at the interfaces of consecutive layers. Such synergistic effects were corroborated by comparing the electrochemical properties of PEDOT films derived from single and multiple polymerization steps (*i.e.* 1-layered and multi-layered PEDOT films, respectively).<sup>36</sup> Again, both the ability to store charge and electrochemical stability were higher for multi-layered films than for 1-layered ones.

In this work we present a multi-optimization process for preparing PEDOT/Al<sub>2</sub>O<sub>3</sub> composites with high *SC* using a simple *in situ* anodic polymerization technique. For this purpose, the influence of the alumina content, the pH of the generation medium and the presence of the synergistic effects associated to multi-layered systems, on the electrochemical properties of the composites have been investigated. Besides, the influence of such parameters in the surface morphology, the surface topography and the wettability has been also examined.

## METHODS

**Materials.** 3,4-Ethylenedioxythiophene (EDOT) monomer from Aldrich and alumina from Panreac were used as received. Anhydrous LiClO<sub>4</sub>, analytical reagent grade from Aldrich, was stored in an oven at 70 °C before use in electrochemical experiments. Acetonitrile solvent, hydrochloric acid and sodium hydroxide were purchased from Sigma Aldrich. Milli-Q water grade (0.055 μS/cm) was used in all synthetic processes.

***Inorganic particles diameter and zeta- ( $\zeta$ )-potential.*** The diameter of alumina particles in EDOT aqueous solutions was determined by dynamic light scattering (DLS). Measurements were performed at room temperature with a NanoBrook Omni Zeta Potential Analyzer from Brookhaven Instruments Corporation using 10 and 40 mM alumina aqueous suspensions at all the investigated pHs. The  $\zeta$ -potential was determined by performing 30 consecutive measurements of 1:1 and 4:1 EDOT:alumina samples at each investigated pH.

***Synthesis of PEDOT and PEDOT/Al<sub>2</sub>O<sub>3</sub>.*** Both anodic polymerization and electrochemical assays were performed with a potentiostat-galvanostat Autolab PGSTAT101 equipped with the ECD module (Ecochimie, The Netherlands) using a three-electrode compartment cell under nitrogen atmosphere (99.995% pure) at room temperature. Steel AISI 316 sheets of 2×2 and 2×1 cm<sup>2</sup> in area were used as working and counter electrodes, respectively. To prevent interferences during the electrochemical assays, the working and counter electrodes were cleaned with acetone and ethanol before each trial. The reference electrode was an Ag|AgCl electrode containing a KCl saturated aqueous solution (offset potential versus the standard hydrogen electrode,  $E^0 = 0.222$  V at 25°C), which was connected to the working compartment through a salt bridge containing the electrolyte solution.

PEDOT films were prepared by chronoamperometry (CA) under a constant potential of 1.10 V. The cell was filled with 50 mL of a 10 mM EDOT aqueous solution at pH of 2.3, 4.0, 7.0, 8.8 or 10.8 containing 0.1 M LiClO<sub>4</sub> as supporting electrolyte. Before conducting the anodic polymerization of EDOT to produce PEDOT films, the overall solution was stirred at 500 rpm for 40 min and purged with nitrogen. PEDOT/Al<sub>2</sub>O<sub>3</sub> films were obtained using identical conditions with exception of the alumina particles, which were added to the generation medium following a 1:1 or 4:1 EDOT: alumina

ratio. The polymerization time,  $\theta$ , was kept fixed at 180 s for PEDOT and PEDOT/Al<sub>2</sub>O<sub>3</sub>.

The electrochemical properties of conventional 1-layered (1L) films were compared with those of 3-layered (3L) systems, which were obtained applying the layer-by-layer electropolymerization technique. More specifically, 3L-PEDOT/Al<sub>2</sub>O<sub>3</sub> were produced using the experimental conditions described for 1L-PEDOT/Al<sub>2</sub>O<sub>3</sub> but applying three polymerization steps of  $\theta = 60$  s each one (*i.e.* the total polymerization time was identical for 3L-films,  $3 \times 60$  s = 180 s, than for 1L-ones).

**Electrochemical characterization.** All electrochemical assays were performed in acetonitrile with 0.1 M LiClO<sub>4</sub> as supporting electrolyte. Cyclic voltammetry (CV) assays were performed to evaluate the *SC* and the electrochemical stability of the composites. The initial and final potentials were -0.5 V, and the reversal potential was 1.6 V. A scan rate of 100 mV/s was used. In this work the electrochemical stability was evaluated by conducting 50 consecutive cycles.

The *SC* (in F/g) was determined from the registered voltammograms using the following Eq:

$$SC = \frac{Q}{\Delta V \cdot m} \quad (2)$$

where  $Q$  is the voltammetric charge,  $\Delta V$  is the potential window (in V), and  $m$  is the mass of polymer on the surface of the working electrode (in g).

Galvanostatic charge/discharge (GCD) curves between 0.2 and 0.8 V were run. The cycling stability was determined by repeating the GCD test during 100 consecutive cycles. The current was adjusted to provide charge and discharge times in the range between 5 and 30 seconds.<sup>37</sup> The charge to 0.8 V was performed at 5 mA during 20 seconds and the discharge to 0.2 V at 1 mA during 10 s.

Moreover, GCD profiles were also used as alternative method to measure the  $SC$ :

$$SC = \frac{i\Delta t}{\Delta V} \quad (3)$$

where  $i$  is the current intensity and  $\Delta t$  is the time interval required for the change in voltage  $\Delta V$ .

The films thickness ( $L$ ) was derived from the mass of polymer deposited in the electrode ( $m_{pol}$ ) using the procedure reported by Schirmeisen and Beck.<sup>38</sup> Accordingly,  $m_{pol}$  was determined with the following relation:

$$m_{pol} = Q_{pol} \left( \frac{m}{Q} \right) \quad (4)$$

where  $Q_{pol}$  is the polymerization charge consumed in the generation of each layer (in  $\text{mC}/\text{cm}^2$ ) and  $m/Q$  is the current productivity (with values in between  $0.45 \pm 0.02$  and  $0.70 \pm 0.06$   $\text{mg}/\text{C}$ , depending on the composition). The volume of polymer deposited in the electrode ( $V_{pol}$ ) was derived from the values of  $m_{pol}$  and the density of PEDOT and PEDOT/ $\text{Al}_2\text{O}_3$ , which was determined using the flotation method.

***Morphological and topographical characterization.*** Scanning electron microscopy (SEM) studies were performed to examine the surface morphology of PEDOT and PEDOT/ $\text{Al}_2\text{O}_3$  films. Dried samples were placed in a Focussed Ion Beam Zeis Neon 40 scanning electron microscope operating at 3 kV, equipped with an energy dispersive X-ray (EDX) spectroscopy system. EDX analyses were performed to identify the presence of alumina at the surface of PEDOT/ $\text{Al}_2\text{O}_3$  films.

Atomic force microscopy (AFM) images were obtained with a Molecular Imaging PicoSPM using a NanoScope IV controller under ambient conditions. The tapping mode AFM was operated at constant deflection. The row scanning frequency was set to 1 Hz. AFM measurements were performed on various parts of the films, which provided reproducible images similar to those displayed in this work. The scan window sizes

used in this work were  $5 \times 5 \mu\text{m}^2$ . The statistical application of the NanoScope Analysis software was used to determine the root mean square roughness ( $R_q$ ), which is the average height deviation taken from the mean data plane.

The distribution of alumina in composites was examined by transmission electron microscopy (TEM) using a Phillips TECNAI 10 transmission electron microscope at an accelerating voltage of 100 kV. For this purpose, small trips of composites were removed from the electrodes with a razor blade and, according the manufacturer protocol, embedded in a low viscosity modified Spurr epoxy resin and curing at  $60^\circ\text{C}$  for 24 h. Ultra-thin sections (less than 100 nm) of these samples were cut at room temperature using a Sorvall Porter-Blum microtome. Finally, the sections were placed on carbon coated cooper grids. Bright field micrographs were taken with a SIS Mega View II digital camera.

**Wettability.** Contact angle measurements were performed to examine the influence of alumina in the wettability of PEDOT. Measurements were carried out using sessile water drop method at room temperature and controlled humidity. Images of  $0.1 \mu\text{L}$  distillate water drops on film surfaces were recorded after stabilization ( $\sim 10$  s) with the equipment OCA 20 (DataPhysics Instruments GmbH, Filderstadt). The software SCA20 was used to analyse the images and acquire the contact angle value. Contact angle values were obtained as the average of 15 independent measures for each sample.

**Thermogravimetry (TGA).** The thermal stability of the prepared samples was studied by TGA at a heating rate of  $20^\circ\text{C}/\text{min}$  (sample weight *ca.* 5 mg) with a Q50 thermogravimetric analyser of TA Instruments and under a flow of dry nitrogen. Test temperatures ranged from  $30$  to  $600^\circ\text{C}$ .

## RESULTS AND DISCUSSION

### ***Preparation of alumina aqueous dispersions***

The solubility of aluminum oxides, hydroxides and oxihydroxides in aqueous solutions depends on the pH because of the aggregation phenomena induced by the surface charges.<sup>21,22</sup> However, the characteristic pH intervals that typically define the physical properties of aqueous alumina dispersions<sup>22</sup> (e.g. particle size distribution, surface charge and sedimentation) are expected to be altered by the presence of EDOT monomer during the *in situ* anodic polymerization. Moreover, such properties will have a deep impact in the interfacial interaction between the alumina and the polymer matrix in PEDOT/Al<sub>2</sub>O<sub>3</sub> composites, as has been observed for other systems involving insulating and electrochemical inactive polymers.<sup>39</sup>

Considering the amphoteric behaviour of Al<sub>2</sub>O<sub>3</sub>, 1:1 and 4:1 EDOT:alumina aqueous dispersions were prepared at pH= 2.3, 4.0, 7.0, 8.8 or 10.8. Thus, the oxide groups at the water/alumina interface are expected to protonate or deprotonate depending on the contacting solution pH,<sup>40,41</sup> even though EDOT monomers may interfere causing some deviations with respect to reported behaviour. Figure 1a presents the dependence of  $\zeta$ -potential of alumina as a function of the pH and the EDOT:alumina ratio. The  $\zeta$ -potential indicates the stability of the colloidal dispersion (*i.e.* resistance towards aggregation), reflecting the degree of electrostatic repulsion between adjacent particles in the dispersion. The physical stability of an aqueous dispersion is considered good when the  $\zeta$ -potential is around +25 or -25 mV.<sup>42</sup> The highest stability of the 1:1 EDOT:alumina dispersion is obtained in acidic conditions, the  $\zeta$ -potential values measured at pH= 2.3 and 4.0 being +23 and -25 mV, respectively. The  $\zeta$ -potential obtained at pH= 8.8 (7 mV), which is the closest to the isoelectric point of Al<sub>2</sub>O<sub>3</sub> (pH= 9.2), reflects the tendency towards aggregation due to van der Waals inter-particle attraction. Interestingly, when the concentration of alumina decreases, the dispersion

becomes stable in the whole examined pH interval. Thus, for the 4:1 EDOT:alumina ratio, the  $\zeta$ -potential is +18 mV for pH= 2.3 and lower than -21 mV for pH $\geq$  4. According to these results, the 4:1 EDOT:alumina ratio provides the most favourable polymerization conditions in terms of stability. Besides, the sedimentation of the 4:1 dispersion is also affected by the pH. More specifically, the precipitation time increases by  $\sim$ 7 min at acid or basic pHs with respect to the neutral one, the slowest sedimentation being obtained at the extremes pH values (2.3 and 10.8).

The variation of the average effective diameter ( $D_{eff}$ ) of alumina aggregates, as determined by DLS, with the pH is displayed in Figure 1b for both 1:1 and 4:1 EDOT:alumina ratios. As it can be seen, average  $D_{eff}$  values are fully consistent with the  $\zeta$ -potential measures represented in Figure 1a. Thus,  $D_{eff}$  increases with the van der Waals inter-particle attraction and the reduction of the electrostatic repulsions, the maximum value (1.2  $\mu$ m) being reached at neutral pH. Besides, although the similarity of the two profiles reflects similar aggregation behaviour, at a given pH  $D_{eff}$  is systematically higher for the 1:1 dispersion than for the 4:1 one. This effect has been attributed to the fact that collisions among particles, which are followed by aggregation rather than by increasing dispersion, increase with the alumina concentration.

Figure 2a displays a representative SEM micrograph of alumina particles deposited onto an AISI 316 sheet from an aqueous dispersion at pH= 7. As it can be seen, irregular particles are widely and randomly distributed onto the steel surface, their size being extremely variable (from more than 10  $\mu$ m to 50 nm). For example, the diameter of particles marked with a white circle in the micrograph is 0.8  $\mu$ m, 100 nm and 9  $\mu$ m (from left to right). Figure 2b displays AFM images of an alumina particle deposited onto steel, which is perfectly identifiable by the phase contrast. The 3D topographic

image reflects the irregular shape of the particle, which exhibits a length and a height of  $\sim 2.3 \mu\text{m}$  and  $\sim 650 \text{ nm}$ , respectively.

Overall, results evidence that EDOT behaves as a dispersant, especially when its concentration is higher than that of alumina. Thus, in absence of dispersants alumina forms stable colloidal solutions at  $\text{pH} < 7.8$ , and The stability decreases on approaching the isoelectric point with maximum instability at  $\text{pH} = 9.1$ .<sup>22</sup> However, 4:1 EDOT:alumina solutions are very stable at  $\text{pH} = 8.8$  and  $10.8$ , the average  $D_{\text{eff}}$  estimated for alumina particles at such basic media being similar to that obtained at  $\text{pH} = 4.0$  and  $2.3$ , respectively.

#### ***Composition of PEDOT/Al<sub>2</sub>O<sub>3</sub> films***

Densities were measured considering all the tested pHs (five samples per system). The average values were  $1.664 \pm 0.009$ ,  $1.679 \pm 0.007$  and  $1.667 \pm 0.009 \text{ g/cm}^3$  for PEDOT, 1:1 PEDOT/Al<sub>2</sub>O<sub>3</sub> and 4:1 PEDOT/Al<sub>2</sub>O<sub>3</sub>, respectively. The small standard deviations indicate that the influence of pH in the composition is very small. Thus, the maximum difference between the highest and lowest density obtained for PEDOT, 1:1 PEDOT/Al<sub>2</sub>O<sub>3</sub> and 4:1 PEDOT/Al<sub>2</sub>O<sub>3</sub> was lower than 1.2%, 1.0% and 1.1%, respectively.

Figure 3 represents the variation of the composition, expressed as Al<sub>2</sub>O<sub>3</sub> w/w (%), as a function of the pH for 1:1 and 4:1 PEDOT:Al<sub>2</sub>O<sub>3</sub>. As it can be seen, the incorporation of Al<sub>2</sub>O<sub>3</sub> is very low at  $\text{pH} = 2.3$  ( $\leq 0.05 \text{ w/w } \%$ ), while the maximum inorganic loading is achieved at the most basic pH (i.e. 0.73 and 1.45 w/w % for 4:1 and 1:1 nanocomposites, respectively). In spite of its low amount, inorganic particles provide a very remarkable benefit (e.g. the SC of PEDOT increases more than twice), as will be shown in next sub-sections.

### *Morphological and thermal characterization of PEDOT/Al<sub>2</sub>O<sub>3</sub> films*

Comparison of representative SEM micrographs recorded for PEDOT and PEDOT/Al<sub>2</sub>O<sub>3</sub> films reveals that the concentration of alumina and the pH do not alter drastically the surface morphology of the CP. Figures 2c-d, which compare PEDOT obtained at pH= 7 with PEDOT/Al<sub>2</sub>O<sub>3</sub> prepared using a 1:1 ratio at pH= 10.8 (both using a polymerization time of 180 s), indicate that the compact globular morphology of PEDOT is preserved in the composite. This similarity suggests that alumina is homogeneously distributed inside the polymer matrix, producing small changes in the general aspect of the surface morphology. Indeed, the micrograph recorded for PEDOT/Al<sub>2</sub>O<sub>3</sub> (Figure 2d) shows a single alumina particle (diameter: 0.9 μm) at the displayed surface, which reflects that such superficial distribution is relatively infrequent. This is corroborated in Figure 2e, which shows a representative SEM micrograph with low magnification.

On the other hand, low magnification micrographs indicate that PEDOT/Al<sub>2</sub>O<sub>3</sub> films display well-localized and prominent folds (height: 1.4 μm according to the topographic AFM image displayed in Figure 2f) homogeneously distributed. The folds on the surface of these films, which are not observed for pure PEDOT films, have been attributed to the alumina particles embedded into the polymeric matrix. These particles act as crystallization nuclei of polymeric and oligomeric chains, promoting the formation of elongated folds. This hypothesis is supported by TEM images, which enables the identification of alumina particles inside the polymeric matrix (Figure 2g). Furthermore, the particles size is fully consistent with those determined in the previous sub-section (Figure 1b).

Figure 4a represents the variation of the contact angle for PEDOT and PEDOT/Al<sub>2</sub>O<sub>3</sub> against the pH of the generation medium. As it can be seen, the influence of the pH in the wettability is relatively small in all cases, contact angle values being comprised between 40° and 51°. Thus, inorganic particles do not cause important changes in the hydrophilicity of PEDOT, which is consistent with the fact that alumina is mainly embedded into the polymeric matrix.

Although details on the thermal decomposition mechanism of PEDOT were already described,<sup>10</sup> the influence of generation conditions (*i.e.* pH and EDOT:alumina ratio) in the thermal stability of the ICP was examined by TGA. Figure 4b displays the thermogravimetric profiles recorded for PEDOT and 1:1 PEDOT/Al<sub>2</sub>O<sub>3</sub> produced at representative pHs. For pristine PEDOT, the thermal decomposition shifts towards lower temperatures when the pH becomes basic and, especially, acid. The onset of the thermal decomposition of alumina-containing composites depends considerably on the pH of the generation medium. Interestingly, the thermal stability of the composite is lower than that of pure PEDOT at basic pH, whereas it is higher at acid pH. Moreover, the thermal stability of pristine PEDOT and PEDOT/Al<sub>2</sub>O<sub>3</sub> obtained at pH= 7.0 and 8.8, respectively, are practically identical. This result represents an important advantage since composites prepared at pH= 8.8 display the best electrochemical performance, as is described in the next sub-section.

#### ***Electrochemical characterization of PEDOT/Al<sub>2</sub>O<sub>3</sub> films***

Table 1 compares the *SC* values determined by GCD (Eq 3) and CV (Eq 2) for pure 1:1 and 4:1 PEDOT/Al<sub>2</sub>O<sub>3</sub> with those pure PEDOT at the investigated pHs. As it was expected, tendencies displayed by galvanostatic and potentiostatic *SC* values, which were obtained using the 5<sup>th</sup> GCD cycle and the 2<sup>nd</sup> voltammogram, respectively, are

fully consistent. Thus, the  $SC$  is higher for PEDOT/ $Al_2O_3$  than for pure PEDOT, independently of the pH and the EDOT:alumina ratio, evidencing that alumina particles improve considerably (in some cases more than twice) the electrochemical performance of the ICP. Based on previous studies devoted to examine the conductivity enhancement of electrolytic media upon the addition of  $Al_2O_3$ ,<sup>43</sup> we propose that the surface groups of the alumina particles provide additional sites for the migration of charges, favouring the mobility of the dopant agents during the charge-discharge and oxidation-reduction processes. Moreover, the enhancement of the  $SC$  increases with the concentration of alumina in all cases with exception of the composites prepared at pH= 8.8. For the latter, the  $SC$  of 4:1 composite is ~7% higher than that of 1:1.

The distinctive behaviour of composites prepared at pH= 8.8 has been attributed to the combination of two different phenomena. First, the  $SC$  of pure PEDOT is significantly higher at pH= 8.8 than at the rest of the examined pHs, which indicates that such moderately basic environment activates the ICP promoting its electrochemical performance. This is probably due to the fact that at pH= 8.8 the concentration of  $OH^-$  groups is high enough to promote their participations as secondary doping agents but too low for degrading the polymeric matrix (as probably occurs at pH= 10.8). Second, the root mean square roughness ( $R_q$ ) is different for films yielded using 1:1 and 4:1 EDOT:alumina ratios, as it is proved by the AFM images compared in Figure 5. More specifically,  $R_q = 77 \pm 3$ ,  $80 \pm 5$  and  $91 \pm 3$  nm for PEDOT, 1:1 and 4:1 PEDOT/ $Al_2O_3$ , respectively. The topography of 4:1 films can be described as a uniform distribution of sub-micrometric protuberances with well-defined separations (*i.e.* dissemination of mountains separated by narrow valleys), while the AFM image of the 1:1 film displays a single protuberance of micrometric dimensions in terms of length, width and height. This observation, which is fully consistent with the stability of 1:1 and 4:1

EDOT:alumina dispersions discussed above (Figure 1a), explains that  $R_q$  is higher for the 4:1 film, even though the maximum roughness ( $R_{max}$ ) is higher for the 1:1 film ( $R_{max}= 623$  and  $539$  nm for 1:1 and 4:1 films, respectively). Although these differences do not affect the general aspect of the surface morphology (Figure 2), they have a notable effect in the capacity of the films to exchange ions. Thus, the  $SC$  increases with the specific surface of the films and, therefore, with  $R_q$ .

Figure 6a compares the first five GCD cycles recorded at  $1.53$  A/g y  $1.67$  A/g of 1:1 and 4:1 PEDOT/ $Al_2O_3$ , respectively, prepared at  $pH= 8.8$  using a  $0.1$  M  $LiClO_4$  acetonitrile solution as electrolytic medium. The GCD curves present some distortions with respect to the typical triangular shape, which are caused by the voltage drop ( $V_{drop}$ ) and the voltage gain ( $V_{gain}$ ) at the beginning of the discharging and charging process, respectively. Although the curves are very similar for the two PEDOT/ $Al_2O_3$  composites, the  $V_{drop}$  is slightly higher for the 1:1 than for the 4:1, which is in agreement with the  $SC$  values listed in Table 1. Figure 6b shows the 2<sup>nd</sup> cyclic voltammogram in  $0.1$  M  $LiClO_4$  acetonitrile recorded for 4:1 PEDOT/ $Al_2O_3$  samples prepared at different pHs. As it can be seen, the first oxidation peak of PEDOT chains,  $O_1$ , occurs between  $0.3$  and  $0.5$  V, depending on the pH, while the second peak,  $O_2$ , overlaps with the oxidation potential of the medium. In addition, two reduction peaks,  $R_1$  and  $R_2$ , are detected in the cathodic scans, indicating the presence of redox pairs in the recorded potential range. These redox processes, which are well-defined for all the pHs employed during the generation of the films, should be attributed to the formation of polarons in the polymer chains.

Figure 6c indicates that, after 200 GCD of cycles, the  $SC$  remains practically constant for all PEDOT and PEDOT/ $Al_2O_3$  electrodes, independently of their preparation conditions, indicating that very small changes are expected for a larger number of

cycles. The  $SC$ s determined by CV before and after 50 consecutive oxidation-reduction cycles reflect a decrease of around 50%-60% for both PEDOT and PEDOT/ $Al_2O_3$  (Figure 6d). Apparently, these drastic reductions, which occur in the first 20 redox cycles, are in contradiction with the results displayed in Figure 6c for the galvanostatic  $SC$  values. However, it should be emphasized that application of consecutive oxidation–reduction cycles is the most aggressive electrochemical method to determine the electrochemical stability of polymeric films. This was proved in previous studies, in which potentiostatic redox cycles were found to reduce drastically the porosity and roughness of PEDOT films, affecting their surface topography and morphology.<sup>8,45</sup> Besides, it should be noted that, after the reduction occurred during the first 20 redox cycles, the order of the potentiostatic  $SC$  values remains identical to that obtained after the 2<sup>nd</sup> redox cycle. Accordingly, in spite of all films are affected by the potentiostatically-induced degradation, the electrochemical stability is higher for PEDOT/ $Al_2O_3$  than for PEDOT at all the examined pHs.

Table 2 compares the thickness of PEDOT and PEDOT/ $Al_2O_3$  films, which was estimated considering the polymerization charge, the current productivity and the density for each generation condition. As it was expected, the thickness is lower for pure PEDOT than for PEDOT/ $Al_2O_3$  in all cases. This should be attributed to the steric hindrance caused by the inorganic particles, which increases with the content of  $Al_2O_3$  in the film (*i.e.* the thickness of 1:1 composite is the highest). On the other hand, the thickness increases with the polymerization charge, reflecting again that the influence of the pH in the amphoteric behaviour of  $Al_2O_3$ .

### ***Electrochemical advantages of multilayered PEDOT/ $Al_2O_3$ films***

The potential advantages of 3L-PEDOT films, which were yielded using three polymerization steps of 60 s each one, with respect to single layered (1L) PEDOT systems described above, which were obtained using a continuous electropolymerization process of 180 s, are reflected in Figure 7. As it can be seen, both the galvanostatic and potentiostatic *SCs* are higher for 3L-films than for 1L-films, independently of the pH. Moreover, this ranking does not change with increasing number of cycles, the electrochemical stability being higher for the former than for the latter in all cases. Accordingly, observations for PEDOT films prepared in water are fully consistent with our previous results on films prepared in acetonitrile.<sup>36</sup> This behaviour has been attributed to the interfaces created at the interlayer regions during the multi-step polymerization. Thus, such interfaces, which are not present in films prepared using a continuous electropolymerization process, act as dielectric layers, enhancing the ability to store charge.

Besides, the galvanostatic / potentiostatic *SC* of yielded at pH= 8.8 increases from 91 / 97 F/g to 105 / 115 F/g, respectively, when the number of layers increases, which represents an enhancement of 15% / 18 %. These remarkable increments corroborate that the application of multiple polymerization steps at pH= 8.8 result in the combination of two favourable effects: *i*) the creation of dielectric layers inside the PEDOT films; and *ii*) the activation of PEDOT chains through the OH<sup>-</sup> groups arising from the basic generation medium, as discussed in the previous sub-section.

The galvanostatic and potentiostatic *SCs* values determined for 3L-PEDOT/Al<sub>2</sub>O<sub>3</sub> films are compared with those obtained using a single polymerization step in Figures 7a and 7b, respectively. As it can be seen, for a given experimental conditions, 3L-films exhibit higher the ability to store charge than 1L-films. The increment induced by the interfaces formed between composite layers ranges from 2% to 13%, depending on the

pH, the EDOT:alumina ratio and the methodology used to determine the *SC* (*i.e.* GCD or CV). This interval of variation is in good agreement with that obtained from the comparison of pure 1L- and 3L-PEDOT films prepared in acetonitrile (*i.e.* the average increment of the ability to store charge was 9%), reflecting the synergistic effects induced by the interfaces.<sup>36</sup> The galvanostatic *SC* of 3L-PEDOT/Al<sub>2</sub>O<sub>3</sub> films remains practically unaltered after 200 GCD cycles, independently of the pH and the feeding ratio, as is illustrated in Figure 8c for 1:1 and 4:1 3L-films obtained at pH= 8.8. In opposition, the potentiostatic *SC* values determined for 3L-films decreases around 45%-55% after 50 consecutive redox cycles (Figure 8d). This behaviour, which is independent of the pH (not shown) is similar to that displayed in Figure 6d for single layered films.

## CONCLUSIONS

We successfully synthesized PEDOT/Al<sub>2</sub>O<sub>3</sub> composites in aqueous medium by CA considering different monomer:alumina ratios in the reaction medium, pHs ranging from 2.3 to 10.8, and both continuous and multi-step *in situ* polymerization strategies. Independently of the selected synthetic conditions, the electrochemical properties for energy storage of PEDOT/Al<sub>2</sub>O<sub>3</sub> are better than those of pure PEDOT, which has been attributed to the additional sites for the migration of charges provided by the alumina particles. Analyses of the properties of the initial EDOT:alumina suspensions and synthesized composites show that the best properties are obtained applying a multi-step polymerization strategy, a 4:1 EDOT:alumina ratio and a pH of 8.8. The success of these conditions results from the combination of four different factors: (i) 4:1 EDOT:alumina suspensions are stable at such basic pH despite it is very close to the isoelectric point of alumina; (ii) the OH<sup>-</sup> groups participate as dopant agents giving an

extra activation to the PEDOT; (iii) the basic pH is still too moderate to promote the degradation of the polymeric matrix; and (iv) the interfaces generated by the multi-step polymerization strategy, which act as a dielectric placed between two polymeric layers, are compatible with incorporation of alumina particles inside the polymer matrix. The PEDOT/Al<sub>2</sub>O<sub>3</sub> composites presented here will be further investigated for their incorporation into solid-state organic supercapacitors based on the combination of PEDOT electrodes and biohydrogels as electrolytic medium. Thus, the replacement of PEDOT by PEDOT/Al<sub>2</sub>O<sub>3</sub> prepared at the above mentioned conditions may lead to improve the performance of these electrochemical energy storage devices introducing a very small amount of non-toxic inorganic material.

## ACKNOWLEDGEMENTS

Authors acknowledge MINECO/FEDER (MAT2015-69367-R) for financial support. M.S.G is grateful to Costa Rica National Commission of Scientific and Technological Research (CONICYT-Support N°FI-172B-14). C.A. is grateful to ICREA Academia program.

## REFERENCES

1. Y. Huang, H. Li, Z. Wang, M. Zhu, Z. Pei, Q. Xue, Y. Huang, C. Zhi, *Nano Energy*. **2016**, *22*, 422–438.
2. C. Janaky, K. Rajeshwar, *Prog. Polym. Sci.* **2015**, *43*, 93–135.
3. B. C. Kim, J. Y. Hong, G. G. Wallace, H. S. Park, *Adv. Funct. Mater.* **2015**, *5*, 1500959.
4. K. Wang, H. Wu, Y. Meng, *Small* **2014**, *10*, 14–31.

5. N. P. S. Chauhan, M. Mozafari, N. S. Chundawat, K. Meghwal, R. Ameta, S.C. Ameta, *J. Ind. Eng. Chem.* **2016**, *36*, 13–29.
6. A. J. Heeger. *Angew. Chem. Int. Ed.* **2001**, *40*, 2591–2611.
7. D. Aradilla, F. Estrany, C. Alemán *J. Phys. Chem. C.*, **2011**, *115*, 8430–8438.
8. J. Wang, Z. Wu, H. Yin, W. Li, Y. Jiang, *RSC Adv.* **2014**, *4*, 56926–56932.
9. D. Aradilla, D. Azambuja, F. Estrany, M. T. Casas, C.A. Ferreira, C. Alemán, *J. Mater. Chem.* **2012**, *22*, 13110–13122.
10. X. Bai, X. Hu, S. Zhou, *RSC Adv.* **2015**, *5*, 43941–43948.
11. Y. Shi, L. Peng, G. Yu, *Nanoscale* **2015**, *7*, 12796–12806.
12. M. M. Pérez-Madrigal, F. Estrany, E. Armelin, D. Díaz-Díaz, C. Alemán, *J. Mater. Chem. A* **2016**, *4*, 1792–1805.
13. W. B. Guo, X. D. Zhang, X. Yu, S. Wang, J. Qiu, W. Tang, L. Li, H. Liu, Z. L. Wang, *ACS Nano* **2016**, *10*, 5086–5095.
14. C. Chen, T. Zhang, Q. Zhang, X. Chen, C. Zhu, Y. Xu, J. Yang, J. Liu, D. Sun, *ACS Appl. Mater. Interfaces* **2016**, *8*, 10183–10192.
15. W. Lee, Y. H. Kang, J. Y. Lee, K-S. Jang, S. Y. Cho, *RSC Adv* **2016**, *6*, 53339–53344.
16. R. Ramakrishnan, S. J. Devaki, S. Thomas, M. R. Varma, K. P. P. Naajiya, *J. Phys. Chem. C.* **2016**, *120*, 4199–4210.
17. C. X. Guo, G. Yilmaz, S. Chen, S. Chen, X. Lu, *Nano Energy* **2015**, *12*, 76–87.
18. Z. H. Wang, P. Tammela, J. Huo, P. Zhang, M. Strømme, L. Nyholm, *J. Mater. Chem. A* **2016**, *4*, 1714–1722.
19. D. López-Pérez, D. Aradilla, L. J. Del Valle, C. Alemán, *J. Phys. Chem. C* **2013**, *117*, 6607–6619.
20. G.V. Franks, L. Meagher, *Colloids Surf. A* **2003**, *214*, 99–110.

21. B. P. Singh, R. Menchavez, C. Takai, M. Fuji, M. Takahashi, *J. Colloid Interface Sci.* **2005**, *291*, 181–186.
22. S. Kirchmeyer, K. Reuter, *J. Mater. Chem.* **2005**, *15*, 2077–2088.
23. R. Xiao, S. Il. Cho, R. Liu, S. B. Lee, *J. Am. Chem. Soc.* **2007**, *129*, 4483–4489.
24. R. Liu, S. B. Lee, *J. Am. Chem. Soc.* **2008**, *130*, 2942–2943.
25. Y. Shirai, S. Takami, S. Lasmono, H. Iwai, T. Chikyow, Y. Wakayama, *J. Polym. Sci., Part B: Polym. Phys.* **2011**, *49*, 1762–1768.
26. R. Liu, S. Il. Cho, S. B. Lee, *Nanotechnology* **2008**, *19*, 215710.
27. C. R. Martin, *Science* **1994**, *266*, 1961–1966.
28. R. V. Parthasarathy, C. R. Martin, *Chem. Mater.* **1994**, *6*, 1627–1632.
29. C. R. Martin, *Acc. Chem. Res.* **1995**, *28*, 61–68.
30. M. Steinhart, J. H. Wendorff, A. Greiner, R. B. Wehrspohn, K. Nielsch, J. Schilling, J. Choi, U. Gosele, *Science* **2002**, *296*, 1997–1997
31. D. Aradilla, F. Estrany, R. Oliver, C. Alemán, *Eur. Polym. J.* **2010**, *46*, 2222–2228.
32. F. Estrany, D. Aradilla, R. Oliver, E. Armelin, C. Alemán, *Eur. Polym. J.* **2008**, *44*, 1323–1330.
33. D. Aradilla, F. Estrany, E. Armelin, C. Alemán, *Thin Solid Films.* **2010**, *518*, 4203–4210.
34. D. Aradilla, M. M. Pérez-Madrigal, F. Estrany, D. Azambuja, J. I. Iribarren, C. Alemán, *Org. Electron.* **2013**, *14*, 1483–1495.
35. D. Aradilla, F. Estrany, C. Alemán, *J. Appl. Polym. Sci.* **2011**, *121*, 1982–1991.
36. S. K. Ramasahayam, A. L. Clark, Z. Hicks, T. Viswanathan, *Electrochim. Acta* **2015**, *168*, 414–422.
37. M. Schirmeisen, F. J. Beck, *J Appl Electrochem.* **1989**, *19*, 401–409.

38. S. Mallakpour, E. Khadem, *Prog. Polym. Sci.* **2015**, *51*, 74–93.
39. J. Sung, L. Zhang, C. Tian, Y. R. Shen, G. A. Waychunas, *J. Phys. Chem. C* **2011**, *115*, 13887–13893.
40. J. P. Fitts, X. Shang, G. W. Flynn, T. F. Heinz, K. B. Eisenthal, *J. Phys. Chem. B* **2005**, *109*, 7981–7986.
41. N. Mandzya, E. Grulke, *Powder Technol.* **2005**, *160*, 121–126.
42. P. Jayathilaka, M. Dissanayake, I. Albinsson, B-E. Mellander, *Electrochim. Acta* **2002**, *47*, 3257–3268.
43. Z. Wang, X. Huang, L. Chen, *Electrochem. Solid-State Lett.* **2003**, *6*, E40–E44.

**Table 1.** Specific capacitance (*SC*, in F/g) determined by GCD (using the 5<sup>th</sup> cycle) / CV (using the 2<sup>nd</sup> voltammogram) for pure PEDOT and PEDOT/Al<sub>2</sub>O<sub>3</sub> prepared using both 1:1 and 4:1 EDOT:alumina ratios at different pHs.

<b>pH</b>	<b>PEDOT</b>	<b>PEDOT/Al<sub>2</sub>O<sub>3</sub></b>	
		<b>1:1</b>	<b>4:1</b>
2.3	58 / 55	121 / 119	115 / 111
4.0	73 / 67	89 / 91	77 / 82
7.0	58 / 68	- / -	- / -
8.8	91 / 97	132 / 120	141 / 129
10.8	81 / 92	114 / 117	98 / 105

**Table 2.** Thickness ( $L$ ) and polymerization charge ( $Q_{pol}$ ) consumed in the preparation of PEDOT and PEDOT/Al<sub>2</sub>O<sub>3</sub> films at different pHs:  $L$  (in  $\mu\text{m}$ ) /  $Q_{pol}$  (in C)

<b>pH</b>	<b>PEDOT</b>	<b>PEDOT/Al<sub>2</sub>O<sub>3</sub></b>	
		<b>1:1</b>	<b>4:1</b>
2.3	1.180 / 0.430	1.524 / 0.519	1.262 / 0.456
4.0	1.932 / 0.527	2.038 / 0.527	1.957 / 0.470
8.8	1.221 / 0.455	1.487 / 0.515	1.249 / 0.535
10.8	1.841 / 0.590	2.074 / 0.627	1.564 / 0.547

## CAPTIONS TO FIGURES

**Figure 1.** Variation of (a) the  $\zeta$  potential and (b) the effective particle diameter as a function of the pH for 1:1 and 4:1 EDOT:alumina aqueous dispersions.

**Figure 2.** (a) SEM micrograph and (b)  $10 \times 6.3 \mu\text{m}^2$  AFM images (phase, 3D topography and cross-sectional profile at the top, middle and bottom part, respectively) of alumina deposited onto steel AISI 316 from an aqueous dispersion at pH= 7. Alumina particles of very different diameters (0.8  $\mu\text{m}$ , 100 nm and 9  $\mu\text{m}$  from left to right) are marked with white circles in (a). (c) SEM micrograph of PEDOT obtained by anodic polymerization in neutral water (pH= 7) using a polymerization time of 180 s. (d-e) SEM micrographs and (f)  $10 \times 10 \mu\text{m}^2$  3D topographic image of PEDOT/ $\text{Al}_2\text{O}_3$  obtained using a 1:1 EDOT: alumina ratio at pH= 10.8. The infrequent alumina particles localized at the surface are inside the white squares. (g) TEM micrographs of PEDOT/ $\text{Al}_2\text{O}_3$  obtained using the same conditions that in (d-f).

**Figure 3.** Variation of the amount of  $\text{Al}_2\text{O}_3$  (w/w %) in 4:1 and 1:1 PEDOT/ $\text{Al}_2\text{O}_3$  composites as a function of the pH.

**Figure 4.** (a) Variation of the contact angle as function of the pH of the generation medium for PEDOT, 1:1 and 4:1 PEDOT/ $\text{Al}_2\text{O}_3$ . In all cases error bars are smaller than the size of the symbols. (b) Thermogravimetric curves of PEDOT and 1:1 PEDOT/ $\text{Al}_2\text{O}_3$  prepared at the most representative pHs.

**Figure 5.** Representative height AFM images ( $5 \times 5 \mu\text{m}^2$ ) of PEDOT, 1:1 and 4:1 PEDOT/ $\text{Al}_2\text{O}_3$  obtained at pH= 8.8

**Figure 6.** (a) Five GCD cycles recorded from 0.2 to 0.8 V for 1:1 and 4:1 PEDOT/ $\text{Al}_2\text{O}_3$  prepared at pH= 8.8. (b) Cyclic voltammogram (2<sup>th</sup> cycle) recorded from -0.5 to 1.6 V at a scan rates of 100 mV/s for 4:1 PEDOT/ $\text{Al}_2\text{O}_3$  prepared at pH= 2.3, 4.0, 8.8 and 10.8. (c-d) Variation of the SC with the number of (c) GCD and (d) CV

cycles for PEDOT, 1:1 and 4:1 PEDOT/Al<sub>2</sub>O<sub>3</sub> prepared at pH= 2.3, 4.0, 8.8 and 10.8. All electrochemical assays were performed using a 0.1 M LiClO<sub>4</sub> acetonitrile solution as electrolytic medium.

**Figure 7.** Variation of the *SC* with the number of (c) GCD and (d) CV cycles for 1L-PEDOT and 3L-PEDOT prepared at pH= 2.3, 4.0, 8.8 and 10.8. All electrochemical assays were performed using a 0.1 M LiClO<sub>4</sub> acetonitrile solution as electrolytic medium.

**Figure 8.** Comparison of the (a) galvanostatic and (b) potentiostatic *SCs* measured by GCD and CV, respectively, for 1L- and 3L-PEDOT/Al<sub>2</sub>O<sub>3</sub> prepared at different pHs. Variation of the *SC* with the number of (c) GCD and (d) CV cycles for 1L- and 3L-PEDOT/Al<sub>2</sub>O<sub>3</sub> prepared at pH= 8.8. Films prepared using both 1:1 and 4:1 EDOT:alumina ratios have been considered in all cases.

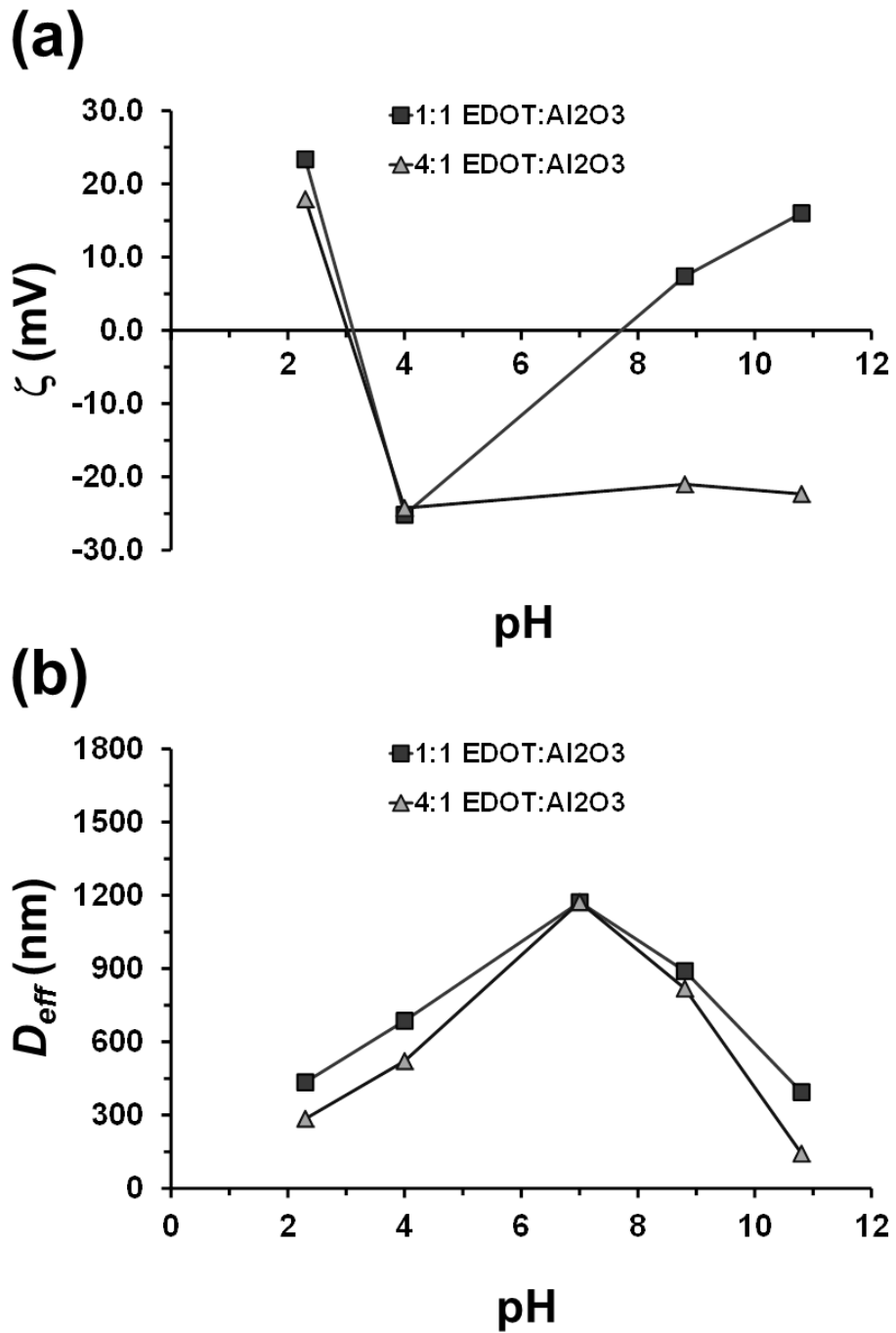


Figure 1

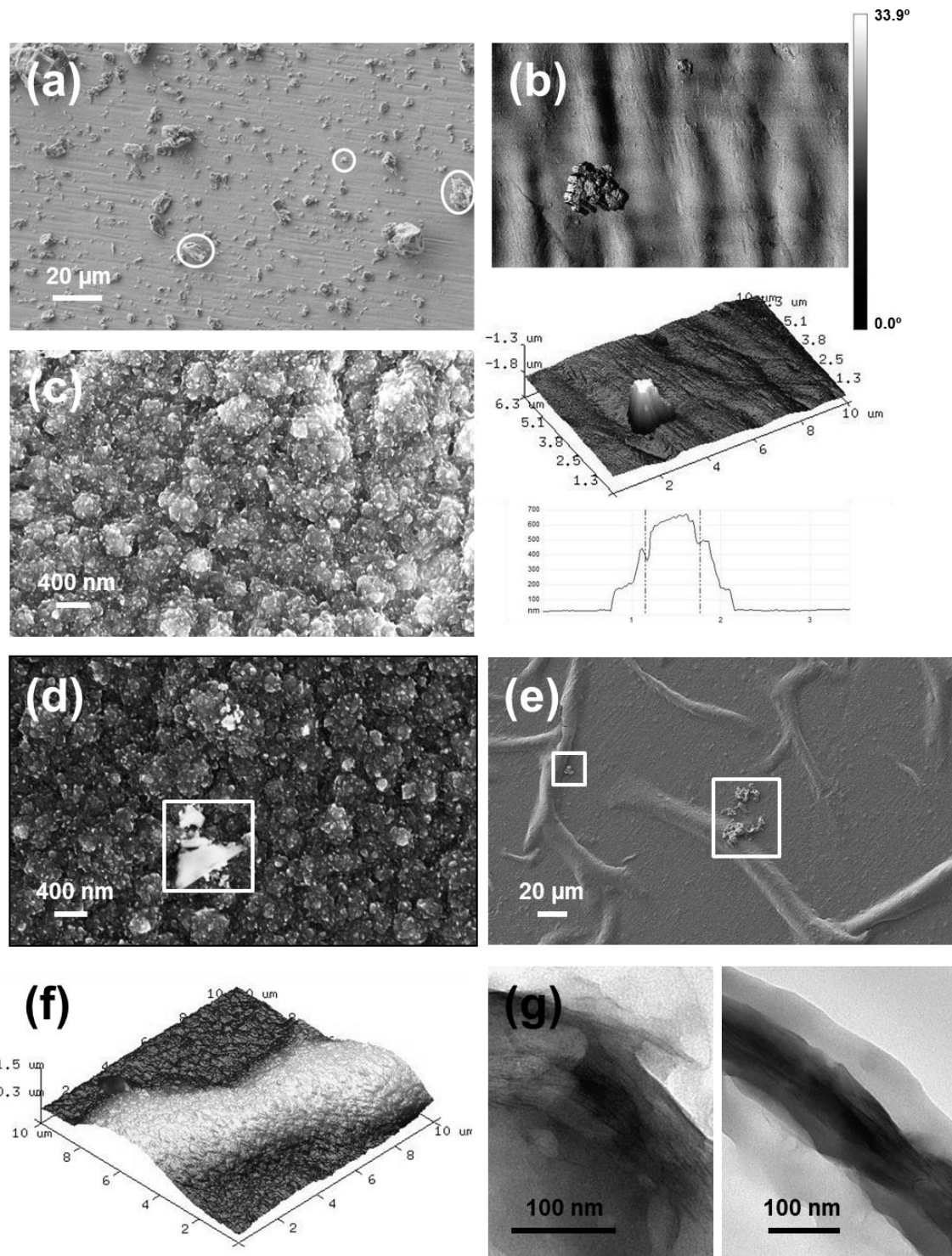


Figure 2

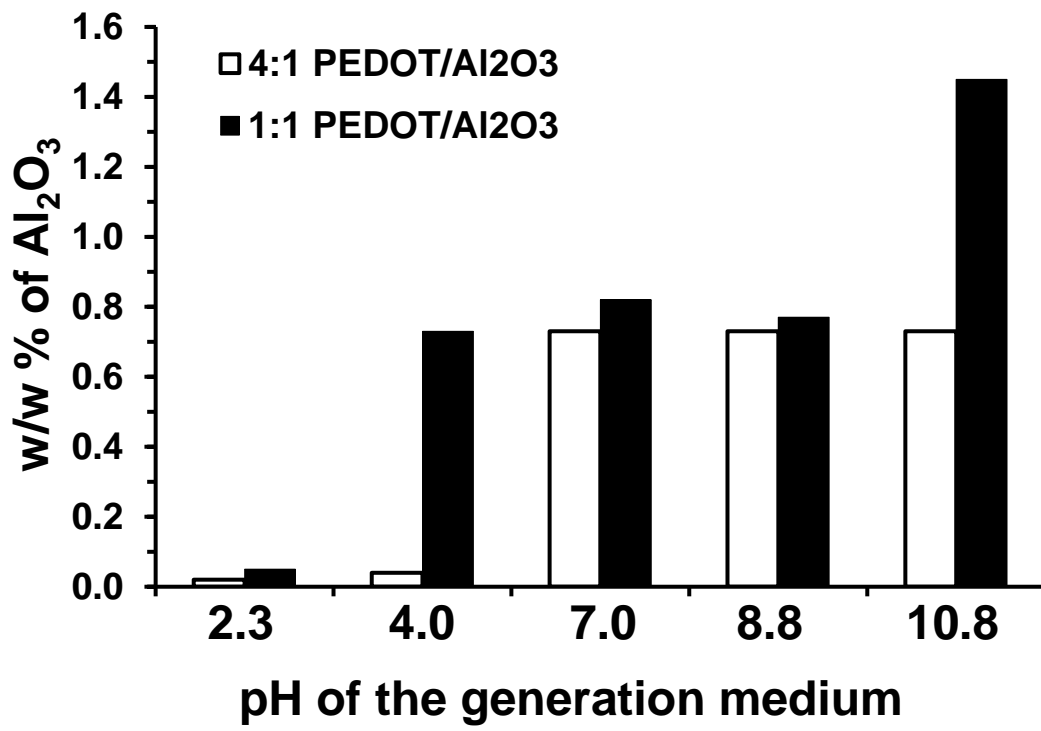


Figure 3

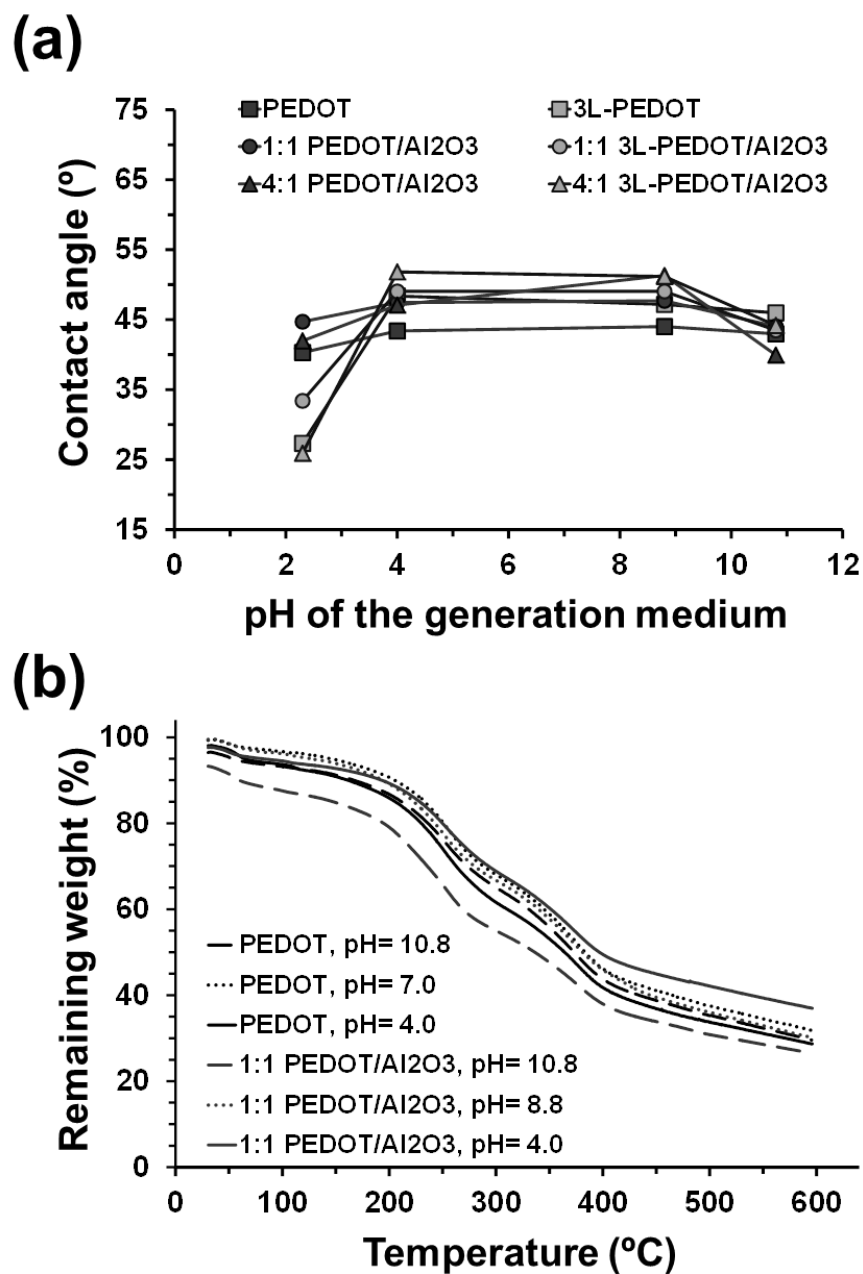


Figure 4

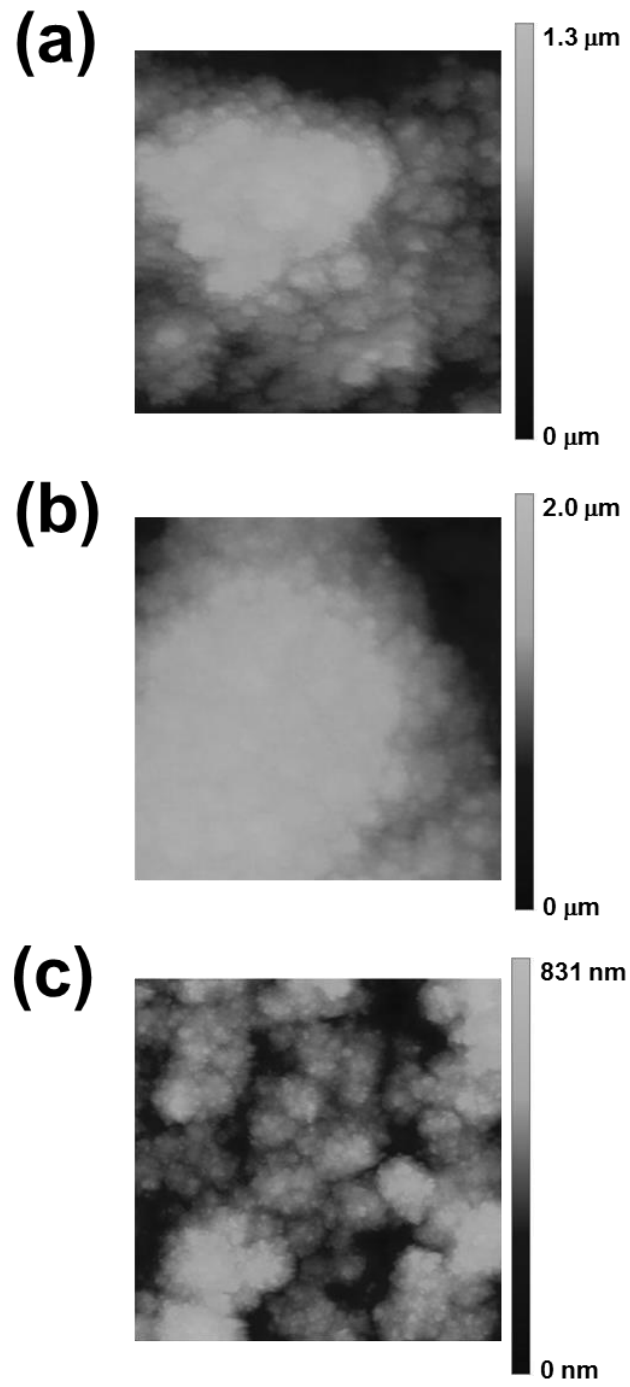


Figure 5

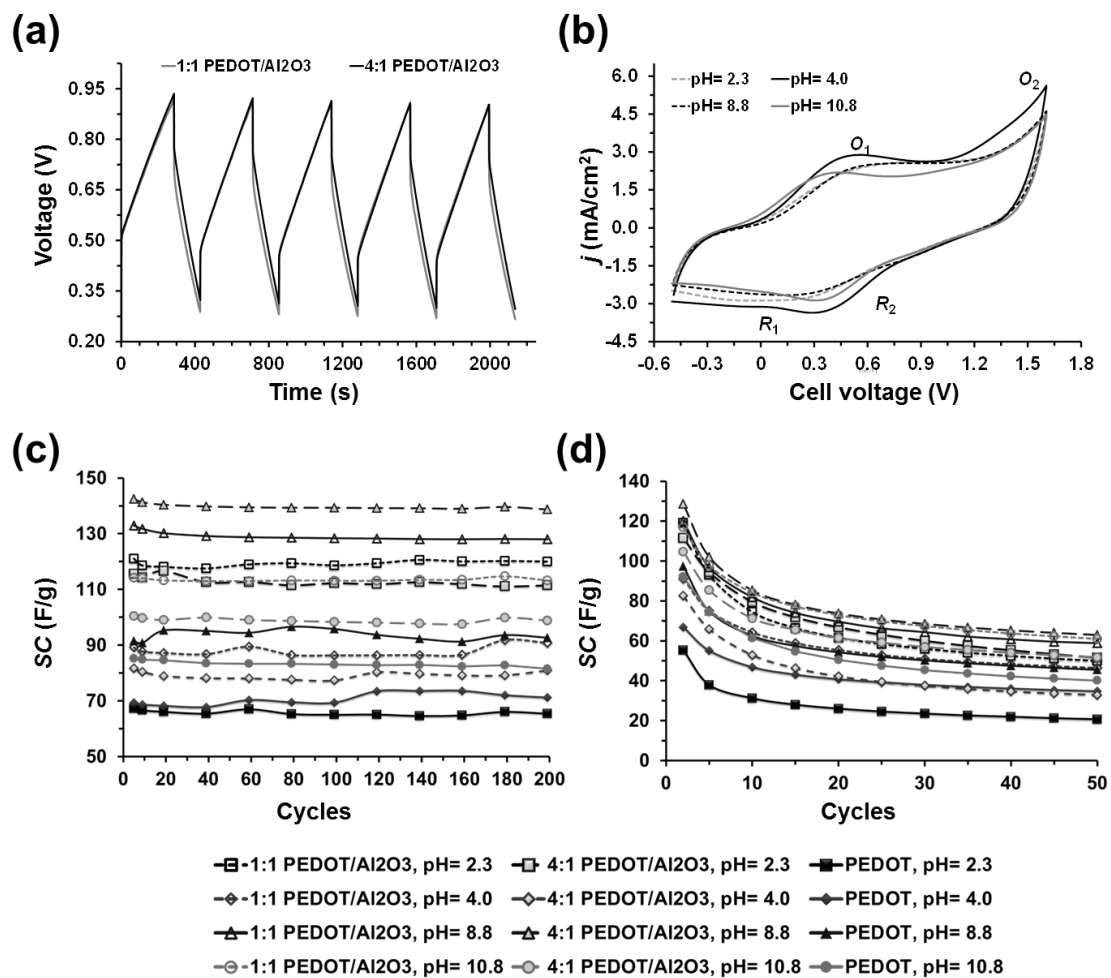
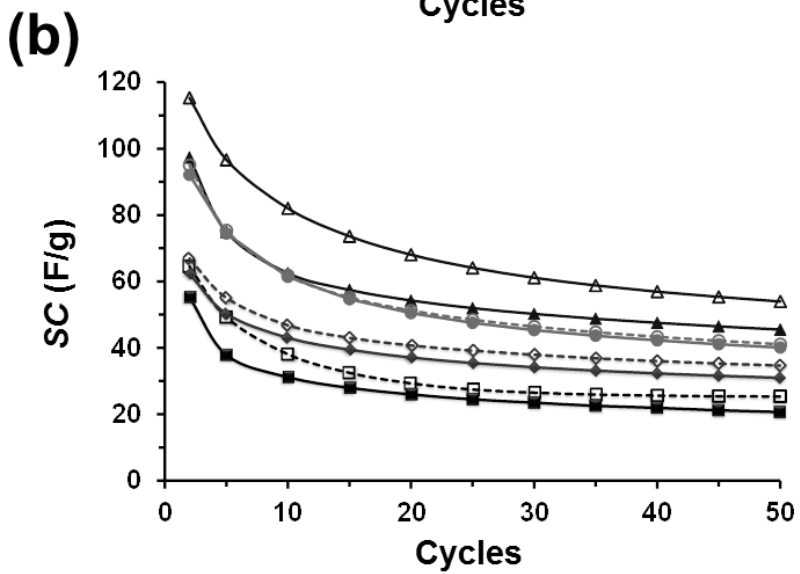
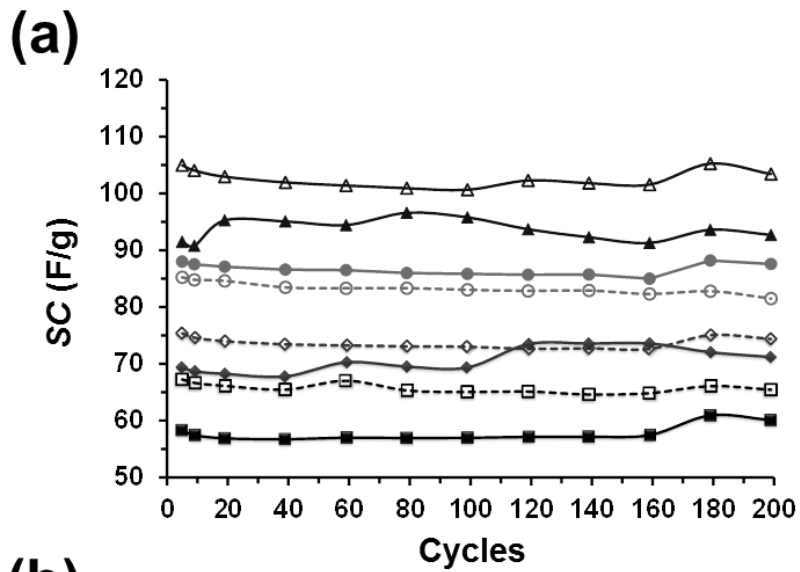


Figure 6



- |                       |                       |
|-----------------------|-----------------------|
| □ -3L-PEDOT, pH= 2.3  | ■ -1L-PEDOT, pH= 2.3  |
| ◇ -3L-PEDOT, pH= 4.0  | ◆ -1L-PEDOT, pH= 4.0  |
| △ -3L-PEDOT, pH= 8.8  | ▲ -1L-PEDOT, pH= 8.8  |
| ○ -3L-PEDOT, pH= 10.8 | ● -1L-PEDOT, pH= 10.8 |

Figure 7

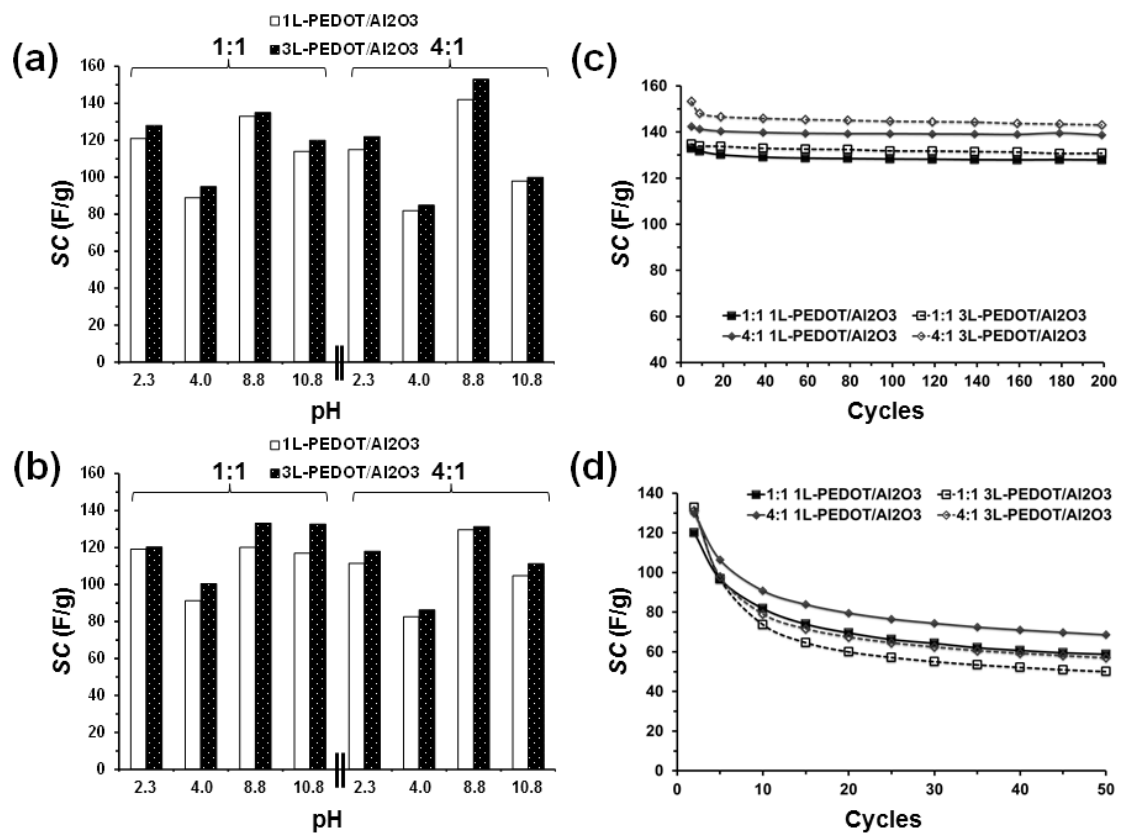


Figure 8

## Graphical Abstract

